

In-Line Characterization of Heterojunction Bipolar Transistor Base Layers by High-Resolution X-Ray Diffraction

N. D. Nguyen^a, R. Loo^a, A. Hikavy^a, B. Van Daele^a,
P. Ryan^b, M. Wormington^b and J. Hopkins^b

^a IMEC, Kapeldreef 75, B-3001 Leuven, BELGIUM

^b Bede plc, Belmont Business Park, Durham, DH1 1TW, UK

The suitability of high-resolution X-ray diffraction (HRXRD) as an in-line measurement tool for the characterization of heterojunction bipolar transistor SiGe base layers and Si cap layers was investigated. We showed that despite of polycrystalline Si on the mask material of patterned wafers, HRXRD measurements performed on an array of small windows yield results which are comparable to those that were obtained on a window which is larger than the size of the source beam, regarding the thickness and the Ge content of the SiGe layers. The possibility to extract layer parameters for active device windows of different sizes was therefore demonstrated. The suitability of HRXRD for in-line measurement of the Si cap thickness was also assessed and the sensitivity of this technique for determining the substitutional boron concentration in SiGe was studied. The detection limit in the monitoring of the active dopant concentration was about $2.7 \times 10^{19} \text{ cm}^{-3}$.

Introduction

The efficient control of the properties of the $\text{Si}_{1-x}\text{Ge}_x$ base layer in heterojunction bipolar transistors (HBT) is a critical requirement in order to optimize the benefit of the $\text{Si}/\text{Si}_{1-x}\text{Ge}_x$ band offset and to achieve high device performance in bipolar complementary metal oxide semiconductor (BiCMOS) technology (1-4). For production applications, layer uniformities in the range of 1 – 2 % are required and reproducibility from one epitaxial growth process to the other one has to be of the same order of magnitude. Layer thickness and layer composition (Ge content) are generally measured by Rutherford backscattering spectroscopy (RBS), secondary ion mass spectrometry (SIMS) or photoluminescence (PL). Although these techniques are very well developed, they are not suitable as production measurement tools : RBS and SIMS are destructive analysis methods and PL requires time-consuming cryogenic processes which limit factory throughput. Alternatively, high-resolution X-ray diffraction (HRXRD) and spectroscopic ellipsometry (SE) allow a fast, non-destructive analysis and are therefore suitable for in-line monitoring. Indeed, it has been demonstrated that SE can be used as an in-situ or ex-situ technique to determine the composition and thickness of either thick, relaxed or thin, strained $\text{Si}_{1-x}\text{Ge}_x$ epitaxial layers while HRXRD is an established technique that can accurately measure strain, composition, relaxation and thickness of $\text{Si}_{1-x}\text{Ge}_x$ layers grown by epitaxial processes (5, 6).

In this work, we assessed the applicability of HRXRD as a production-oriented measurement tool for the characterization of BiCMOS heterostructures. The study was

carried out on both blanket and patterned wafers. It focused on three different applications. In the first application, a wafer was processed with a pattern containing test matrices, with each test matrix consisting of an array of a single window dimension. A SIMS pad, which mimics blanket-like measurement conditions, was included in the pattern. As we report here, although polycrystalline Si is present on the mask material, the interpretation of the ω - 2θ scans performed on an array of small windows leads to similar conclusions as those that are obtained on a window which is larger than the size of the incident X-ray beam. From the point of view of device applications, this means that HRXRD allows to control the epilayer properties for different device sizes.

It is also important that the values of the layer thicknesses are correctly extracted from the analysis of the HRXRD scans. In order to assess the suitability of HRXRD for in-line measurement of the Si cap thickness in HBT base layers, comparison with SE was done on Si/SiGe layer stacks with different deposition times for the growth of the Si-cap. In the third application, the sensitivity of HRXRD for the determination of the substitutional boron concentration in SiGe was investigated. The distortion of the silicon lattice due to doping with boron as a substitutional impurity has been studied since the early days of silicon technology, leading to highly accurate measurements of the lattice contraction coefficient (7-11). In this paper, our aim is to give an estimation of the minimum active boron concentration in SiGe that can be monitored by HRXRD in production environment. For this purpose, measurements of the XRD peak shift for layers with boron content varying within a broad range are needed. Smooth epilayers were fabricated by in-situ doping of SiGe grown by reduced pressure chemical vapor deposition (RPCVD) which resulted in highly homogeneous boron concentrations. The high quality of the epitaxially-deposited films allowed to avoid the difficulties that could be encountered in the interpretation of XRD data of diffused materials with non uniform boron contents (11), and to determine the concentration threshold for HRXRD monitoring with good reliability. Finally, this utility of HRXRD can be exploited in other applications like embedded SiGe which is nowadays used in pMOS devices to boost device performance (12).

The paper is organized as follows. After a description of the growth and characterization procedures, we first present the results obtained by HRXRD on patterned wafers and discuss the comparison between small and large windows as well as comparison with SIMS data. Next the correlation between thickness measurements as extracted from HRXRD and those extracted from SE is discussed. Finally, we demonstrate the ability of HRXRD to monitor the active boron concentration and give an estimation of the threshold value.

Experimental

All epitaxial layers were deposited on 200 mm Si (001) wafers, using a standard horizontal cold wall, load-locked, ASM Epsilon™ 2000 reactor, a RPCVD system designed for production applications. Deposition conditions for non-selective epitaxial growth of Si and Si_{1-x}Ge_x include a pressure of 40 Torr and H₂ as a carrier gas. Silane (SiH₄) and germane (GeH₄, 1 % diluted in H₂) were used as Si and Ge source gases, respectively, while diborane (B₂H₆, 50 ppm or 1 % diluted in H₂) was used as source gas for boron (B). For patterned wafers, a combination of 20 nm oxide capped with 60 nm nitride was utilized as mask material. The test matrices of the pattern have dimensions of

270 $\mu\text{m} \times 270 \mu\text{m}$ whereas the dimensions of the open windows varied from 0.18 μm to 10 μm in both directions. Before deposition, the blanket wafers received a $\text{NH}_4\text{OH}/\text{O}_3$ -based clean followed by an in-situ bake at 1050°C for 60 seconds in H_2 in order to remove the native oxide. For patterned wafers, the pre-deposition treatment consisted in a $\text{NH}_4\text{OH}/\text{O}_3$ -based clean followed by a HF 2% dip during 30 seconds and an in-situ bake at 850°C for 2 minutes. Because of the non-selective conditions of the growth, deposition occurs simultaneously in the open Si windows (epitaxial growth) and on the mask material (growth of polycrystalline layers) (13).

HRXRD measurements were performed using a BedeMetrix™-L tool from Bede X-ray Metrology fitted with a Microsource™ micro-focus source, a ScribeView™ optic and a channel-cut beam conditioning crystal. The beam cross-section at the sample position was less than 100 $\mu\text{m} \times 100 \mu\text{m}$. The angular position ω of the sample axis and that of the detector axis, 2θ , were adjusted with respect to the incident X-ray beam using a high-precision goniometer (6). The background intensity was less than 0.3 counts per second (cps). The analysis of the HRXRD spectra was performed using the RADS 4.0 software, a simulation and data-fitting program from Bede X-ray Metrology (14, 15). SE measurements were made with an Advanced Spectroscopic Ellipsometry Technology (ASET-F5) system from KLA-TENCOR, which is a production-oriented completely automated small-spot (30 $\mu\text{m} \times 30 \mu\text{m}$) spectroscopic ellipsometer. The polarizer rotates continuously and the analyzer is fixed in position of each measurement. The SE technique consists of measuring the ($\tan \Psi$, $\cos \Delta$) spectra, which are collected as function of wavelength in the range 250 – 750 nm from the integrated intensity reaching the detector in each 45° octant of the polarizer's rotation, and performing a mathematical regression analysis using the harmonic oscillator model developed by C. Ygartua and M. Liaw (16). Within this method, single $\text{Si}_{1-x}\text{Ge}_x$ epilayers and $\text{Si}/\text{Si}_{1-x}\text{Ge}_x$ layer stacks can be studied and layer thicknesses as well as Ge contents can be determined (5). By comparison with stepheight measurements, the accuracy of the determined thicknesses is about 2 %. The SIMS was performed on an Atomika 4500 depth profiler. Measurement conditions consisted of 500 eV O_2^+ bombardment at 0° incidence.

Results and Discussion

First we discuss the results obtained on patterned wafers, the open windows of which have been filled with an epitaxially-deposited full HBT base layer. HRXRD data measured from an array of small windows are compared to those measured from a large pad and to SIMS results. The conclusions of this work will give the motivation for the next experiment which consists in comparing the values of the Si-cap thickness measured by HRXRD, SE and SIMS. In the last part, we will discuss the monitoring of the boron concentration by means of HRXRD and determine the threshold concentration for the active boron.

Determination of Layer Thickness and Ge Content of HBT Layers Deposited on Patterned and Unpatterned Wafers with Non Selective Growth Conditions

In the open windows, the typical full base layer stack for HBT in BiCMOS applications contains a first epitaxial $\text{Si}_{1-x}\text{Ge}_x$ layer (labeled L1) deposited on the Si substrate, followed by a second $\text{Si}_{1-x'}\text{Ge}_{x'}$ layer (labeled L2) with $x' < x$. A boron spike doping is included in the first $\text{Si}_{1-x}\text{Ge}_x$ layer. The stack is capped by a pure Si layer

(labeled L3). On the mask material, the RPCVD process conditions resulted in the growth of polycrystalline material. The compositional analysis was done on a large ($270\ \mu\text{m} \times 270\ \mu\text{m}$) open area of the pattern (SIMS pad). The Si, Ge and B concentrations as function of depth are shown in Figure 1a.

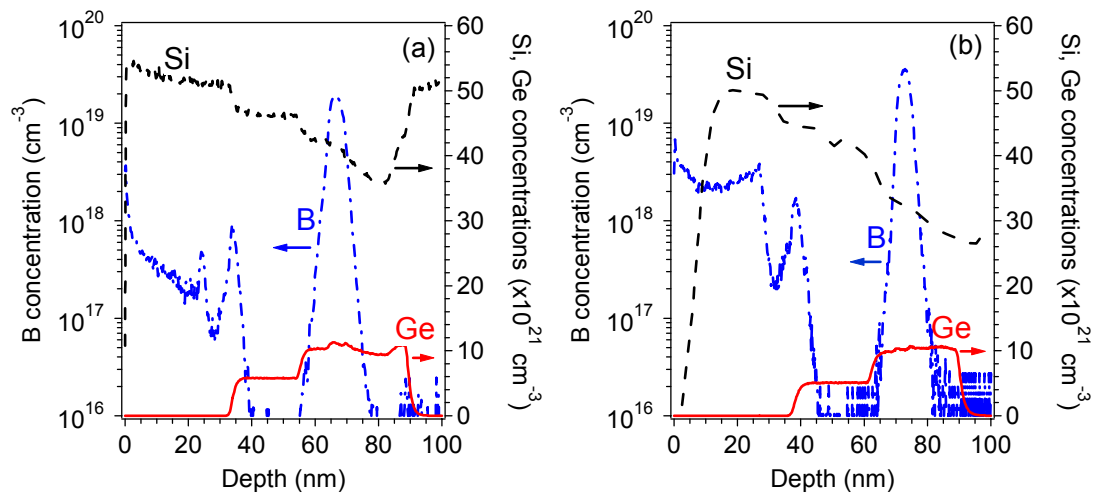


Figure 1. Concentrations of Si, Ge and B in the base layer of a typical npn HBT as function of depth, as measured by SIMS, (a) in the SIMS pad of a patterned wafer and (b) on a blanket wafer.

As expected from the definition of the deposition sequence, two steps are present in the Ge curve. Since the goal is to check the correlation between different characterization techniques for the determination layer thickness and layer composition, the design of the base in this work does not include any ramped Ge layer although graded Ge alloying in the base allows to reduce the transit time by forming an accelerating field for the minority carriers (17). In Figure 2a, the anomalies in Si and Ge profiles are due to charging effects and do not have any impact on the thickness values. The boron profile shows a main peak in layer L1 at 66.5 nm from the surface with a magnitude of $2 \times 10^{19}\ \text{cm}^{-3}$ and a full width at half magnitude (FWHM) of 4.8 nm. For the determination of the thicknesses, we applied the following cutoff condition, which is widely used, to the Ge profile: the boundary between two adjacent layers is defined as the depth coordinate at which the Ge concentration is the average of their values. Prior to this, the nominal Ge concentration in layers L1 and L2 were calculated by averaging the data points of each plateau. The results of the analysis are shown in Table I. The typical error relative to thickness estimation from given SIMS profiles is about 0.2 nm.

Figure 2 shows typical 004 ω - 2θ scans from an array of $5\ \mu\text{m} \times 5\ \mu\text{m}$ wide windows (Figure 2a) and from a $270\ \mu\text{m} \times 270\ \mu\text{m}$ SIMS pad (Figure 2b). The latter one corresponds to a virtual measurement on blanket wafer. The scans exhibit two main different diffraction peaks; the most intense and narrowest peak corresponds to the Si substrate while the broader structure containing interference fringes can be attributed to the SiGe layers. The HRXRD data were analyzed using dynamical diffraction theory and an automated data-fitting algorithm embedded in RADS software from Bede X-ray Metrology (14, 15). Agreement between experiment and best-fit simulation of the $\text{Si}/\text{Si}_{1-x}\text{Ge}_x/\text{Si}_{1-x}\text{Ge}_x$ epitaxial structure is very good.

| | | Patterned wafer | | | Blanket wafer | |
|-------------------|----|---|-------------------|------|------------------|------|
| | | HRXRD on 5 $\mu\text{m} \times 5 \mu\text{m}$ | HRXRD on SIMS pad | SIMS | HRXRD | SIMS |
| Thickness (nm) | L3 | 39.6 \pm 0.4 | 41.2 \pm 0.2 | 34.4 | 37.2 \pm 0.4 | 38.0 |
| | L2 | 21.8 \pm 0.3 | 23.4 \pm 0.2 | 22.0 | 22.3 \pm 0.3 | 25.6 |
| | L1 | 33.8 \pm 0.3 | 36.3 \pm 0.1 | 34.0 | 27.2 \pm 0.3 | 26.8 |
| Ge (%) | L2 | 6.26 \pm 0.12 | 6.45 \pm 0.06 | | 7.11 \pm 0.06 | |
| | L1 | 13.22 \pm 0.03 | 13.58 \pm 0.02 | | 12.92 \pm 0.03 | |

As shown in Table I, the results obtained for the array of small windows are very similar to those corresponding to the SIMS pad. It must be highlighted here that this correlation was observed despite of the polycrystalline Si present on the mask in the first case. Figure 2 also illustrates that the presence of the non-monocrystalline material does not affect the angular position of the peaks nor the quality of the fit; it only alters the relative intensities. The decrease in the coherently diffracted intensity might lead, in some cases, to the reduction of a peak to a shoulder that cannot be resolved in position. Interference fringes are indeed more visible in the experimental data related to the SIMS pad because a weaker effect of the polycrystalline material is expected. Moreover, concerning layer thicknesses, the fact that the converged values are systematically lower for the small windows measurements than for the large window case are also explained by the general intensity reduction of the broader peaks and interference fringes. Despite the abovementioned remarks, a good overall agreement of the values of the thicknesses and of the Ge contents could be reached between results obtained for the array of 5 $\mu\text{m} \times 5 \mu\text{m}$ windows and those obtained for the large window. From the point of view of device applications, this means that HRXRD can be efficiently used as an in-line characterization technique to monitor epitaxial layer stacks. An efficient control of the epilayer properties for different device sizes is therefore possible with this method.

The comparison with the SIMS results for the SiGe thicknesses shows a good correlation with HRXRD data. This confirms the satisfactory quality of the latter measurements. A significant disagreement between HRXRD and SIMS can however be observed for the Si-cap thickness. The average difference is about 6.0 nm. Such a discrepancy can not be attributed alone to surface transient effects which are known to alter secondary ion yields (18-22). Even if we take into account the full error corresponding to the accuracy of thickness determination from the concentration profiles and add it to the SIMS differential shift, the observed deviation is still too large. This is in contrast with the good correlation that was observed in a similar experiment on blanket wafer. The values of the layer thicknesses and Ge contents for a full HBT layer stack grown on an unpatterned wafer are given in Table I. The concentrations as functions of depth are shown in Figure 1b; here, the measurement of the Si profile was performed with a lower resolution but layer thicknesses can still be determined by the analysis of the Ge profile. The value of the Si-cap thickness as extracted from HRXRD data and that as extracted from SIMS are particularly in very good agreement for the blanket wafer whereas they are significantly different for the patterned wafer. In the latter case, the comparison is done for HRXRD measurement on a large window. In order to clarify this

issue, we designed an experiment to specifically assess the quality of the Si-cap thickness measurement by HRXRD.

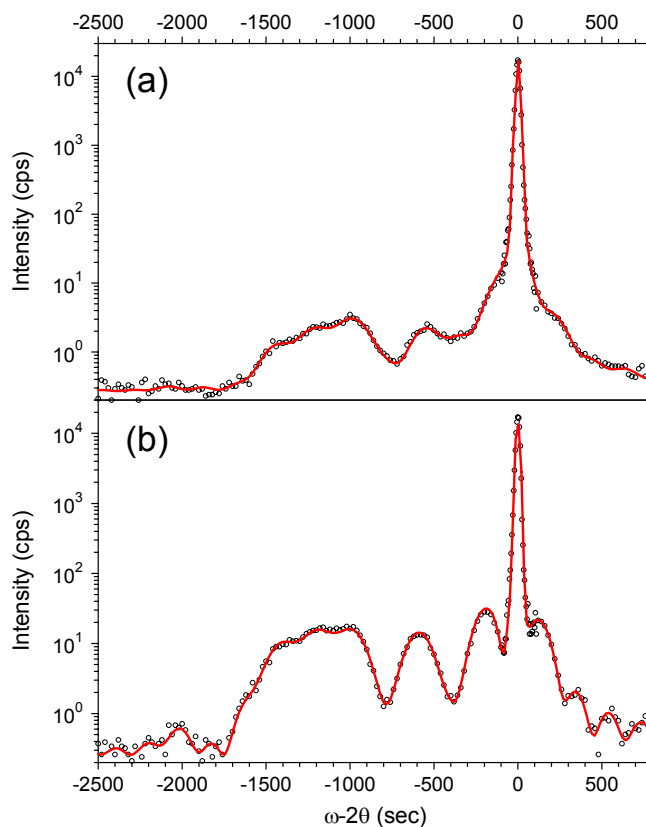


Figure 2. HRXRD scans from (a) a $5\ \mu\text{m} \times 5\ \mu\text{m}$ test pad and (b) a $270\ \mu\text{m} \times 270\ \mu\text{m}$ SIMS test pad. The measured ω - 2θ scans (circles) around the symmetric 004 reflection are shown with their best-fit simulations (full lines).

Determination of the Si-cap Thickness : Comparison Between HRXRD, SE and SIMS

First a single SiGe reference layer was epitaxially grown on p-type Si substrate. Indeed, for our fitting procedure, the layer stack must be restricted to a single-step Ge profile in order to enable SE measurements. Then we fabricated Si/SiGe layer stacks with various Si deposition times. All other growth conditions were identical, including those used for the SiGe layer. Deposition was done on blanket material. From SE characterization of the reference wafer, we obtained an epilayer thickness at the center point of 98.5 nm and a Ge content of 16.2 %. A 49-point line scan measurement gave an average value of 99.7 nm and 16.0 % of Ge. From HRXRD data collected at the center point of the wafer, a Ge content of 16.3 % was determined whereas best-fit simulation yielded a thickness value of 96.3 nm and 16.4 % of Ge. The standard deviation of the layer thickness as measured by the SE line scan was 1.3 %.

The results of the Si-cap thickness measurements are given in Table II. A first batch consisting of 4 wafers (#1 - #4) was fabricated. The SE average values and standard deviation (std dev.) illustrate the good uniformity of the epitaxial deposition whereas single point comparison between HRXRD and SE were done at the center of the wafer. The results show that both techniques are in good agreement regarding the determination

of the Si cap thickness. The discrepancy ranges from 0.8 nm for the thickest (~ 110 nm) Si epilayer to 1.1 nm for the thinnest one (~ 22 nm).

In order to confirm the quality of that correlation, a second batch of 3 wafers (#5 - #7) was processed. A new SiGe reference wafer was used for this run. From single point SE measurement we obtained a value of 89.7 nm for the SiGe thickness and Ge content of 16.3 % at the center of the wafer and an average of 89.2 nm with 16.2 % of Ge was deduced from a 49-point line scan. The SiGe layer was uniform within standard deviation of 0.8 %. The measurements of the Si cap thicknesses of the second batch by the two techniques are included in Table II. Here, the discrepancy ranges from 0.8 nm for the thickest layer to 1.2 nm for the thinnest one.

| Wafer | HRXRD (center) | SE (center) | SIMS | SE (average) | SE std dev. (%) |
|-------|----------------|-------------|------|--------------|-----------------|
| #1 | 21.6 | 22.7 | | 21.5 | 4.5 |
| #2 | 26.3 | 26.2 | | 24.3 | 6.8 |
| #3 | 55.1 | 55.0 | | 54.0 | 2.3 |
| #4 | 110.0 | 109.2 | | 112.9 | 2.4 |
| #5 | 18.5 | 19.7 | 18.6 | 18.6 | 4.1 |
| #6 | 46.8 | 46.4 | 44.7 | 44.0 | 3.5 |
| #7 | 91.8 | 91.0 | 88.4 | 88.5 | 1.9 |

Figure 3 shows a graphical summary of the results. It illustrates the excellent correlation between HRXRD and SE for the evaluation of the thickness of the Si cap layer. These experiments clearly demonstrate that the determination of the Si cap thickness by HRXRD is as accurate and reliable as by SE, which has had its reliability demonstrated in literature for the characterization of single SiGe epilayers and Si/SiGe layer stacks (5, 16). SIMS analysis was also performed on wafers #5 to #7 and the cap layer thickness was estimated from the Ge concentration profiles (not shown here); results are given in Table II.

The comparison of HRXRD, SIMS and SE data leads to the observation that overall, there is a good agreement between the three techniques for measurements on blanket materials. For patterned wafers, the discrepancy between HRXRD and SIMS measurements could be explained by a couple of reasons. At the Bragg angle for Si (004), the footprint of the beam is elliptical, the size being doubled in one direction. This can lead to an extension of the incident intensity outside of the SIMS pad and to a decreasing of the signal-on-noise ratio. Furthermore, edge effects might reduce the effective uniform area of the SIMS pad and contribute to the increasing of the background.

Monitoring of the Active Boron Concentration in SiGe by HRXRD

The incorporation of boron at high concentration levels causes a significant lattice distortion of the doped layer with respect to the undoped material, resulting from the smaller covalent radius of boron compared to that of silicon or germanium. The lattice mismatch induces strain and can generate misfit dislocations as well in thick, relaxed layers. In the regime of purely elastic accommodation of the lattice to the incorporated boron, the layer strain depends linearly on the dopant concentration (23, 24). Since a

linear response is desired for any sensitive monitoring, measurement of the peak shift by HRXRD, which is directly related to the strain in the epilayer, proved to be an efficient method to determine the active boron concentration. For in-line characterization, it is necessary to know the concentration range that can be monitored.

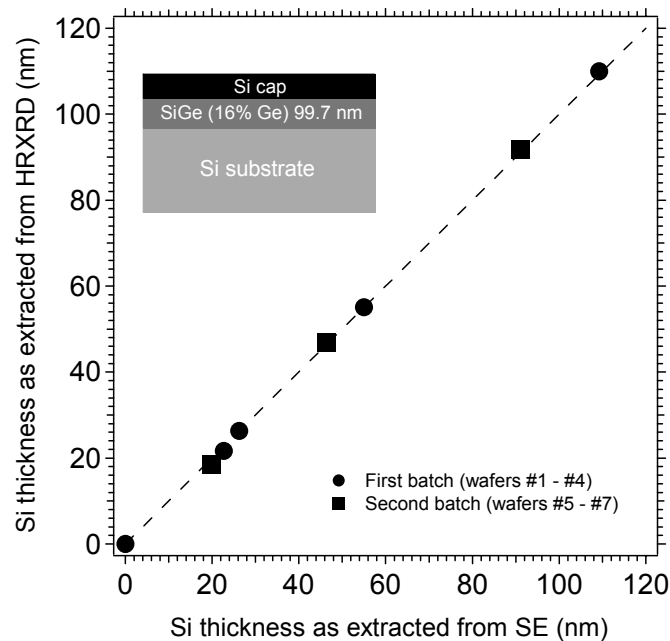


Figure 3. Measurements of the Si cap thickness : comparison between results extracted from HRXRD and those from SE. The layer stack of the first batch is shown as inset. A similar layout was used for the second batch, except for the properties of the SiGe buried layer. The dashed line represents the case of a perfect match between HRXRD and SE.

Therefore, as final application, the sensitivity of HRXRD for monitoring the substitutional boron concentration in SiGe was investigated. An undoped SiGe was first grown. SE measurement performed at the center of the wafer provided a layer thickness of 98.9 nm and Ge content of 16.2 %. From a 49-point line scan, an average thickness of 100.0 nm was measured with a standard deviation of 1.2 % and 16.1 % of average Ge. The best-fit simulation of the HRXRD data provided a thickness value of 96.7 nm and Ge content of 16.4 %. For doped SiGe layers, the control of the active dopant concentration was performed by the flow of the diborane gas. All depositions were made on n-type blanket Si wafers. The substitutional boron concentration for each SiGe:B layer was extracted from the value of the sheet resistance as measured by the four-point probe (4pp) method and by using the average thickness provided by SE. SE and HRXRD were in good agreement regarding the measurement of the undoped and doped SiGe layer thicknesses (not shown here). The Ge content was practically constant for all doping conditions whereas the hole concentration increased with the diborane flow following a power law for moderate concentration values but showing saturation at about $1.6 \times 10^{20} \text{ cm}^{-3}$ obtained for the highest gas flows. This is an indication of the solid solubility of boron in SiGe with Ge content of about 16 %.

The result of the assessment is shown in Figure 4. A linear dependence of the XRD epilayer peak position on the active boron concentration was found for high boron

content whereas for low concentrations, the position of the peak is constant. From the intersection of the linear fit and the averaging, the threshold value is estimated at $2.7 \times 10^{19} \text{ cm}^{-3}$. From SIMS analysis, we deduce that this corresponds to an activation level of about 50 %. The measured concentration profiles allowed to check the very good uniformity of the layer doping. At even higher boron concentrations, the linear trend is not expected to continue as boron would start to precipitate out of solid solution leading to a reduction in the strain gradient with B concentration.

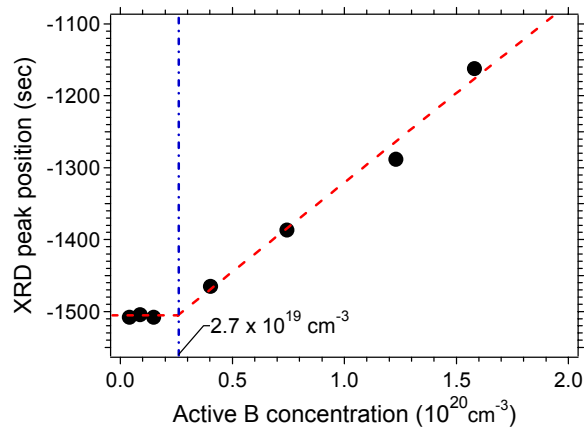


Figure 4. Position of the XRD peak as function of the active boron concentration. Experimental data points are shown in full circles. Dashed lines represent the linear fits and the intersection between the two regions is shown by the dash-dotted line, which corresponds to a threshold concentration of about $2.7 \times 10^{19} \text{ cm}^{-3}$.

Conclusions

In this work, we discussed results of the characterization of HBT base layers by HRXRD and compared the results obtained with those from SE and SIMS measurements. The goal was to assess the suitability of HRXRD as in-line measurement method to monitor Si and SiGe layer thickness as well as layer composition (Ge and B content) in production environment. Specifically for that purpose, HRXRD benefits from several advantages over established techniques. One of them is that it allows for the analysis of the complete HBT layer stack whereas SE is restricted to single SiGe layers or Si/SiGe layer stacks. It is a fast and non-destructive analysis tool that can be readily used to measure small windows on real devices whereas SIMS is limited by a much lower throughput and the device is lost after measurement. We showed that HRXRD measurements of the thickness and Ge content of SiGe layers performed on an array of small windows yield results which are comparable to those that can be obtained on a large window, despite of the presence of polycrystalline Si on the mask material. We also showed that the accuracy of this technique is as good as that of SE concerning the determination of the Si-cap layer thickness on blanket wafers. For patterned wafers, HRXRD measurements led to an overestimation of 6 nm. Finally, the ability of HRXRD to monitor the active boron concentration in SiGe layers was demonstrated for boron contents higher than $2.7 \times 10^{19} \text{ cm}^{-3}$.

Acknowledgments

This work was achieved within the framework of a Joint Development Program between Bede X-ray Metrology and IMEC.

References

1. A. Gruhle, in Proceedings of the 2001 Bipolar/BiCMOS Circuits and Technology Meeting (BCTM), IEEE, p. 19 (2001).
2. R. Loo, M. Caymax, I. Peytier, S. Decoutere, N. Collaert, P. Verheyen, W. Vandervorst, and K. De Meyer, *J. Electrochem. Soc.*, **150**, G638 (2003).
3. P. Wennekers and R. Reuter, in J. D. Cressler, in *Proceedings of the 2004 Bipolar/BiCMOS Circuits and Technology Meeting (BCTM)*, IEEE, p. 79 (2004).
4. J. D. Cressler, in *Proceedings of the 2005 Bipolar/BiCMOS Circuits and Technology Meeting (BCTM)*, IEEE, p. 248 (2005).
5. R. Loo, M. Caymax, G. Blavier, and S. Kremer, *Proc. SPIE 4406*, edited by G. Kissinger and L. H. Weiland, p. 131 (2001).
6. M. Wormington, T. Lafford, S. Godny, P. Ryan, R. Loo, A. Hikavy, N. Bhouri, and M. Caymax, submitted to *Frontiers of Nanoelectronics 2007*.
7. G. L. Pearson and J. Bardeen, *Phys. Rev.*, **75**, 865 (1949).
8. F. H. Horn, *Phys. Rev.*, **97**, 1521 (1955).
9. T. Fukumori, K. Futugami, and K. Matsunaga, *Jpn. J. Appl. Phys.*, **21**, 1525 (1982).
10. H.-J. Herzog, L. Csepregi, and H. Seidel, *J. Electrochem. Soc.*, **131**, 2969 (1984).
11. H. Holloway and S. L. McCarthy, *J. Appl. Phys.*, **73**, 103 (1993).
12. T. Ghani, M. Armstrong, C. Auth, M. Bost, P. Charvat, G. Glass, T. Hoffmann, K. Johnson, C. Kenyon, J. Klaus, B. McIntyre, K. Mistry, A. Murthy, J. Sandford, M. Silberstein, S. Sivakumar, P. Smith, K. Zawadzki, S. Thompson, and B. Bohr, *IEDM Techn. Dig.*, 978 (2003).
13. W. B. de Boer and D. Terpstra, in *Advances in Rapid Thermal Processing*, F. Roozeboom, J. C. Gelpy, M. C. Öztürk, and J. Nakos, Editors, PV 99-10, p. 309, The Electrochemical Society Proceedings Series, Pennington, NJ (1999).
14. D. K. Bowen, L. Loxley, B. K. Tanner, M. L. Cooke, and M. A. Capano, *Mater. Res. Soc. Symp. Proc.*, **208**, 113 (1991).
15. M. Wormington, C. Panaccione, K. M. Matney, and D. K. Bowen, *Phil. Trans. R. Soc. Lond. A*, **357**, 2827 (1999).
16. C. Ygartua and M. Liaw, *Thin Solid Films*, **313-314**, 237 (1998).
17. G. L. Patton, D. L. Hare, J. M. C. Stork, B. S. Meyerson, G. J. Scilla, and E. Ganin, *Electron Device Lett.*, **10**, 534 (1989).
18. Z. X. Jiang, P. F. A. Alkemade, *Surf. and Interf. Analysis*, **27**, 125 (1999).
19. C. W. Magee, G. R. Mount, S. P. Smith, B. Herner, and H.-J. Gossmann, *J. Vac. Sci. and Technol. B*, **16**, 3099 (1998).
20. J. B. Clegg, *Surf. and Interf. Analysis*, **10**, 332 (1986).
21. K. Wittmaack and I. W. Drummond, *Phil. Trans. R. Soc. Lond. A*, **354**, 2731 (1996).
22. W. Vandervorst and F. R. Shepherd, *J. Vac. Sci. Technol. A*, **5**, 313 (1987).
23. M. Wormington, private communication (2007).
24. B. G. Cohen, *Solid State Electron.*, **10**, 33 (1967).